Vibrational Analysis of Nucleic Acids. I. The Phosphodiester Group in Dimethyl Phosphate Model Compounds: $(CH_3O)_2PO_2^-$, $(CD_3O)_2PO_2^-$, and $(^{13}CH_3O)_2PO_2^-$*

Yifu Guan,* Charles J. Wurrey,‡ and George J. Thomas, Jr.*

*Division of Cell Biology and Biophysics, School of Biological Sciences, and ‡Department of Chemistry, University of Missouri–Kansas City, Kansas City, Missouri, USA

ABSTRACT Normal coordinate analyses and vibrational assignments are presented for the dimethyl phosphate anion [$(CH_3O)_2PO_2^-$] and its deuteriomethyl [$(CD_3O)_2PO_2^-$] and carbon-13 [$(^{13}CH_3O)_2PO_2^-$] derivatives in the *gauche-gauche* conformation. The dimethyl phosphate anion, which is the simplest model for the nucleic acid phosphodiester moiety, exhibits many of the spectral complexities of DNA and RNA and has previously resisted a complete and consistent vibrational analysis. In the present study we make use of new experimental data on the dimethyl phosphate isotopomers, including Raman depolarization measurements, to develop a consistent valence force field for normal modes of the C—O—P—O—C phosphodiester network and its hydrogenic substituents, as well as for stretching and bending modes of the O—P—O network of the anionic phosphodioxy group (PO_2^-). The force field established for dimethyl phosphate incorporates one significant nonbonded force constant, introduced from *ab initio* calculations, to account for interaction between the two ester C—O bonds. This study resolves previous problematic assignments for conformation-sensitive symmetric (in-phase) and asymmetric (out-of-phase) skeletal stretching modes of the ester linkages and demonstrates substantial anharmonicity in the hydrogen-stretching vibrations of the methyl substituents. New assignments are proposed for Raman bands of the phosphodioxy group, which may serve as potential indicators of structure and interaction of the DNA phosphates.

INTRODUCTION

Structures of nucleic acid model compounds have been investigated extensively by methods of vibrational spectroscopy. Reviews of the considerable literature on this subject have been given recently (Nishimura and Tsuboi, 1986; Peticolas et al., 1987; Thomas, 1987; Thomas and Tsuboi, 1993). A common goal in these investigations is to establish correlations between vibrational spectra and specific structural features of nucleic acids and their biologically important complexes. Of particular interest are Raman bands that correspond to vibrational modes localized in the nucleic acid phosphodiester group and that are sensitive in frequency or spectral intensity to the conformation of the nucleic acid backbone.

Several examples of conformationally sensitive Raman bands of nucleic acid structures in the A, B, and Z families have been identified (Thomas et al., 1971; Small and Peticolas, 1971; Erfurth et al., 1972; Lafleur et al., 1972; Thamann et al., 1981; Nishimura et al., 1983; Prescott et al., 1984; Thomas et al., 1986; Benevides et al., 1984, 1986, 1988). Libraries of these empirically established conformation indicators have been compiled by Nishimura and Tsuboi (1986), and Thomas and Wang (1988). However, a complete understanding of the vibrational normal modes corresponding to the Raman conformation markers has not yet been achieved. Specifically, the phosphodiester internal coordinates that determine frequency and/or intensity dependence of the Raman bands are not known for any nucleic acid structure.

To address this problem we have undertaken normal coordinate analyses of model compounds representative of the phosphodiester moieties of nucleic acids. Our objectives are to establish reliable assignments for the Raman conformation markers of DNA and RNA and to gain more detailed understanding of the vibrational normal modes. Toward this end we have acquired new experimental data from isotopic derivatives of appropriate phosphodiester analogues, and we have used the Raman and infrared frequencies to develop a valence force field that satisfactorily reproduces the observed vibrational frequencies. We have also made use of *ab initio* calculations to estimate off-diagonal terms of the force-constant matrix. In this initial report, we present our experimental and theoretical results obtained on the simplest nucleic acid phosphodiester analog, dimethyl phosphate (DMP).

A number of experimental and theoretical studies of DMP have been reported. Vibrational spectra of the DMP anion in solution and of various DMP salts in the crystal have been analyzed in conjunction with normal coordinate analyses of the C—O—P—O—C phosphodiester skeleton (Shimanouchi et al., 1964; Garrigou-Lagrange et al., 1976; Okabayashi et al., 1982; Taga et al., 1991). Also, the crystal structure of the ammonium salt of DMP has been described (Giarda et al., 1973), and Monte Carlo calculations have been performed to estimate the relative stabilities of *gauche-gauche*, *gauche-trans*, and *trans-trans* conformers

Received for publication 7 September 1993 and in final form 7 September 1993.

Address reprint requests to Dr. George J. Thomas, Jr., Division of Cell Biology and Biophysics, University of Missouri–Kansas City, 405 Biological Sciences Building, 5100 Rockhill Road, Kansas City, MO 64110-2499.

0006-3495/94/01/225/11 $2.00

of the DMP phosphodiester moiety (Jayaram et al., 1988). These studies are not in complete agreement with one another, regarding either the vibrational assignments or relative stabilities of different DMP conformers. Additionally, key bands in the Raman spectra of DMP remain either unassigned or ambiguously assigned in previous work.

In the present study, we report vibrational spectra of three isotopic forms of DMP, including the normal isotopomer [$(CH_3O)_2PO_2^-$ or DMP-h_6], the deuteriomethyl derivative [$(CD_3O)_2PO_2^-$, DMP-d_6], and the carbon-13 derivative [$(^{13}CH_3O)_2PO_2^-$, DMP-$^{13}C_2$]. These new experimental data resolve ambiguities in previous spectral assignments and serve as the primary basis for the development of a valence force field that satisfactorily reproduces all of the experimentally observed Raman and infrared frequencies. The present results strengthen and extend previous studies and establish a basis for subsequent analyses of the conformational dependence of Raman scattering of DNA and RNA.

MATERIALS AND METHODS

1. Preparation of dimethyl phosphates

Stable isotopes of sodium dimethyl phosphate, for example, NaDMP-h_6, NaDMP-d_6, and NaDMP-$^{13}C_2$, were synthesized using a modification of the method of Noller and Dutton (1933). For preparation of NaDMP-h_6, the phosphorus oxychloride starting material ($POCl_3$; Aldrich, Milwaukee, WI) was converted to trimethyl phosphate, $(CH_3O)_3PO$, by refluxing for 2 h with three equivalents of methanol, and the product was purified by vacuum distillation. The purity of the product was confirmed by comparison of its Raman and infrared spectra with previously published data (Mortimer, 1957). Trimethyl phosphate was then hydrolyzed stoichiometrically to NaDMP with NaOH in an ethanol-water mixture. The NaDMP-h_6 solution was evaporated to dryness, and the solid was washed repeatedly with benzene in accordance with the procedure of McIvor et al. (1956). The product exhibited no Raman bands of either trimethyl phosphate (Mortimer, 1957) or monomethyl phosphate [$(CH_3O)PO_3^{2-}$] (Shimanouchi et al, 1964), indicating >98% purity. For syntheses of NaDMP-d_6 and NaDMP-$^{13}C_2$, methanol-d_3 and methanol-^{13}C (Cambridge Isotope Laboratories, Woburn, MA) were substituted, respectively, for CH_3OH in the above protocol. The products exhibited the same purity as NaDMP-h_6, as judged by the absence from their Raman spectra of bands characteristic of either trimethyl phosphate or monomethyl phosphate anion.

2. Instrumentation and sample handling

a. Raman spectroscopy

Solid samples of NaDMP-h_6, NaDMP-d_6, and NaDMP-$^{13}C_2$, prepared as indicated above, and solution samples prepared at concentrations in the range 0.8–1.0 M in H_2O were sealed in glass capillary tubes (KIMAX no. 34507) and maintained at 25°C for Raman spectroscopy. Raman spectra were excited with the 514.5 nm line of an argon laser (Coherent Innova-70, Santa Clara, CA) using approximately 250 mW of radiant power at the sample. Raman scattering (90° geometry) was collected and analyzed with a computerized Spex Model 1401 double-grating spectrometer, equipped with a single-channel photodetector (Hamamatsu, model R928P). For collection of the parallel and perpendicular components of the polarized Raman spectra of solution samples, a polarizing analyzer and scrambler were located between the sample and entrance slit of the monochromator. Further details of the instrumentation are described elsewhere (Li et al., 1981).

Raman spectra in the 300–3100 cm^{-1} region were collected at 2.0 cm^{-1} intervals with an integration time of 3.0 s, using a spectral slit width of 8 cm^{-1} for solution samples and 4 cm^{-1} for solids. Each spectrum shown below is the average of five to seven scans. The spectral frequencies were calibrated with indene and CCl_4 standards and are believed to be accurate to ±1.5 cm^{-1}.

Spectra of solutions were corrected by subtraction of the weak background of Raman scattering of the aqueous solvent, using procedures described previously (Prescott et al., 1984). For parallel ($I_\parallel$) and perpendicular ($I_\perp$) intensities of the polarized solution spectra, the corresponding polarized spectrum of the solvent was employed in the correction. The solvent-corrected data were processed with SpectraCalc software (Galactic Industries Corp., Salem, NH). Raman band depolarizations ($\rho = I_\perp/I_\parallel$) were calibrated using the totally symmetric stretching vibration of CCl_4, which gave a measured value of $\rho = 0.030$ (corrected to 0.0). Consistent with this correction we observed values of ρ equal to 0.78 for the depolarized bands of CCl_4 at 761 and 791 cm^{-1}. Accuracies of the reported depolarization ratios are estimated to be within ±10% for weak bands and ±3% for strong bands.

b. Infrared spectroscopy

Infrared spectra of NaDMP salts in KBr pellets were recorded with a Mattson Instruments Sirius 100 spectrometer. The spectra in the region from 400 cm^{-1} to 4000 cm^{-1} were collected with the standard high-intensity source, a KBr beam splitter and a liquid nitrogen-cooled mercury cadmium telluride (MCT) detector. Dry nitrogen gas was purged through the spectrometer during the data collection. Generally, 400 scans of the KBr pellet were collected with a spectral resolution of 4 cm^{-1} and triangular apodization function. No baseline corrections were made. Absorption peak positions were determined by taking second derivatives of the original spectra using SpectraCalc software.

3. Calculations

Normal coordinate analyses were carried out on a DECstation 3100 computer (Digital Equipment Corporation, Nashua, NH). The GZINT program, based on the standard Wilson **GF** matrix method, was used for normal coordinate calculations. The program was kindly provided by Professor Richard A. Mathies (Department of Chemistry, University of California, Berkeley).

The **G** matrix was generated using the structural data reported by Newton (1973). The bond lengths are: P–O, 1.48 Å; P—O, 1.61 Å; C—O, 1.42 Å; and C-H, 1.09 Å. (Hereafter, in the text and tables, we use the symbols P–O and P—O to distinguish, respectively, the shorter oxy-anion bond from the longer ester bond of phosphorus. When no symbol is shown, the bond in question should be clear from the context.) The bond angles are: <O–P–O, 119.9°; <O—P—O, 102.6°; <POC, 120.5°; <OCH, 109.5°; and <HCH, 109.5°. Each ester (O—P—O—C) torsion angle (τ) was set at 60°, since crystal structures of DMP salts indicate a strong preference for the *gauche-gauche* (*gg*) conformation, that is, C_2 symmetry (Kyogoku and Iitaka, 1966; Ezra and Collin, 1973; Giarda et al., 1973). The *gg* conformer as well as *gauche-trans* (*gt*) and *trans-trans* (*tt*) conformers are shown in Fig. 1.

The **F** matrix, in terms of a generalized valence force field (GVFF), was constructed from the Urey-Bradley force field (UBFF) reported by Taga et al. (1991). Force constants were converted using the program NCTB, which was generously provided by the late Professor Issei Harada (Pharmaceutical Institute, Tohoku University, Sendai, Japan). Only the diagonal and bonded off-diagonal GVFF force constants were generated from the UBFF **F** matrix; that is, only interactions between bond stretching (or angle bending) coordinates sharing a common atom (or bond) were considered initially. Each normal mode was assigned by GZINT on the basis of the potential energy distribution (PED) in terms of either the force constants or eigenvalues of the secular equation, $|\mathbf{FG} - \lambda\mathbf{E}| = \mathbf{0}$. Both methods gave consistent results. We report the PED in terms of the force constants. The fit of the calculated frequencies to the experimental data was determined using a nonweighted least-squares method.

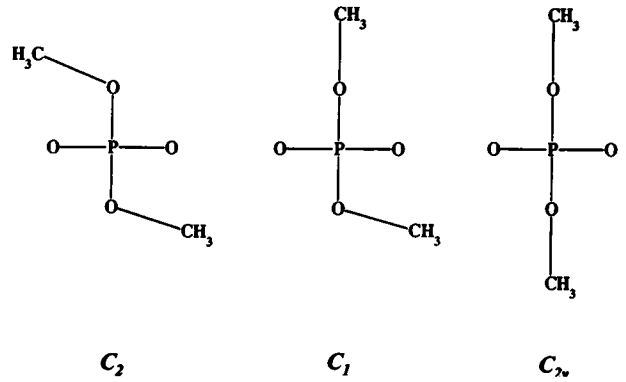

FIGURE 1 Dimethyl phosphate conformers. *Left: gg* conformer (C_2 symmetry). *Middle: gt* conformer (C_1 symmetry). *Right: tt* conformer (C_{2v} symmetry).

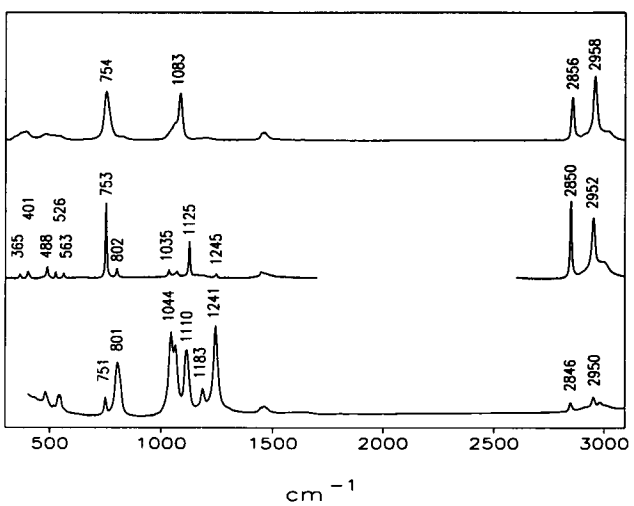

FIGURE 2 Vibrational spectra of NaDMP-h_6. *Top:* Unpolarized Raman spectrum of H_2O solution (0.8 M, pH 7.2). *Middle:* Raman spectrum of polycrystalline solid. *Bottom:* FTIR spectrum of KBr pellet.

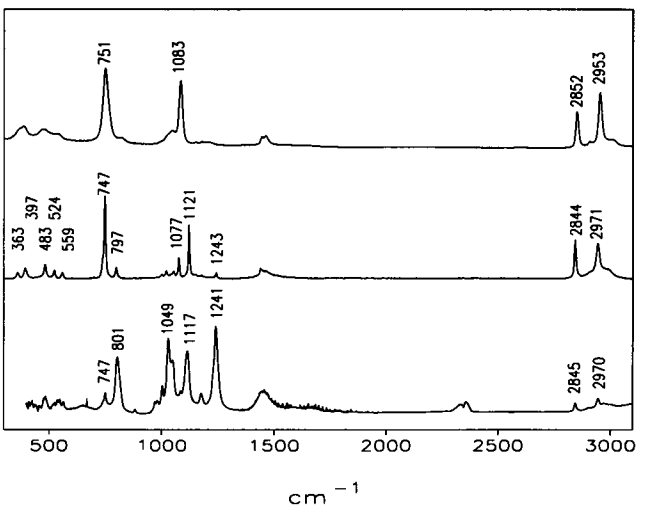

FIGURE 3 Vibrational spectra of NaDMP-$^{13}C_2$. *Top:* Unpolarized Raman spectrum of H_2O solution (0.8 M, pH 7.2). *Middle:* Raman spectrum of polycrystalline solid. *Bottom:* FTIR spectrum of KBr pellet.

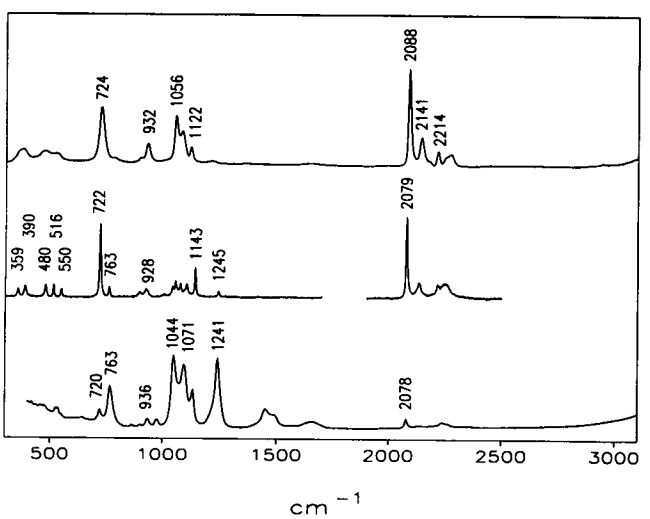

FIGURE 4 Vibrational spectra of NaDMP-d_6. *Top:* Unpolarized Raman spectrum of H_2O solution (0.8 M, pH 7.2). *Middle:* Raman spectrum of polycrystalline solid. *Bottom:* FTIR spectrum of KBr pellet.

RESULTS AND DISCUSSION

1. Spectroscopic data

The unpolarized Raman spectra of solutions of NaDMP-h_6, NaDMP-$^{13}C_2$, and NaDMP-d_6 as well as the Raman and infrared spectra of the corresponding solids are shown in Figs. 2, 3, and 4, respectively. These data are compiled in Tables 1–3 (middle columns). Polarized Raman spectra of H_2O solutions of NaDMP-h_6, NaDMP-$^{13}C_2$, and NaDMP-d_6 are shown in Fig. 5. The Raman frequencies, relative intensities, and depolarization ratios are compiled in the left columns of Tables 1–3. In each table the proposed vibrational assignments are listed in the column on the far right. Further consideration of the experimental data and the basis for the vibrational assignments are given in the following sections.

2. Solution conformation of the dimethyl phosphate anion

The X-ray crystal structures of several dialkyl phosphoesters have been determined and indicate a strong preference for *gg* conformations. The two O—P—O—C torsion angles (τ, τ') in crystal structures of ammonium, magnesium, and barium salts of dialkyl phosphoesters are, respectively, 57.5° and 62.4° (Giarda et al., 1973), 71.6° and 68.2° (Kyogoku and Iitaka, 1966), and 77.6° and 87.4° (Ezra and Collin, 1973). The *gg* conformer has also been proposed for the solution structure of the DMP anion on the basis of vibrational spectra and normal mode analyses (Shimanouchi et al., 1964). On the other hand, Garrigou-Lagrange et al. (1976) concluded from their analysis of the vibrational spectra of DMP and diethyl phosphate (DEP) that *gt* and *tt* states were highly populated. This latter view does not appear to be supported by theoretical calculations. Both *ab initio* molecular orbital calculations and Monte Carlo methods (solvated DMP) strongly favor the *gg* conformation over both *gt* and *tt* (Newton, 1973;

TABLE 1 Vibrational spectra* and assignments‡ of NaDMP-h_6

Raman					Infrared		
Solution			Solid		Solid		
σ	I	ρ	σ	I	σ	I	Assignment
3021	w	(0.6)			3012	w	$\nu_a(CH_3)$
2997	w	(0.7)	2998	sh	2981	w	$\nu_a(CH_3)$
2958	s	0.02	2952	s	2950	w	$\nu_s(CH_3)$
2918	sh	0.23	2918	sh			
2856	s	0.02	2850	s	2846	w	
1464	m	0.78	1469	w	1461	w	$\delta_a(CH_3)$
1450	m	0.49	1449	w	1446	w	$\delta_s(CH_3)$
1217	w	0.64	1245	w	1241	s	$\nu_a(PO_2^-)$
1192	w	0.74	1191	m	1183	m	$r(CH_3)$
1159	w	0.73	1162	w			$r(CH_3)$
1083	s	0.05	1125	s	1110	s	$\nu_s(PO_2^-)$
1058	sh	(0.2)	1070	w	1064	s	$\nu_s(CO)$
1037	sh	(0.7)	1035	w	1044	s	$\nu_a(CO)$
827	w	0.65	802	w	801	s	$\nu_a(OPO)$
754	s	0.03	753	s	751	m	$\nu_s(OPO)$
539	w	0.70	563	m	551	m	$r(PO_2^-)$
503	sh	0.48	526	m	520	w	$\delta(PO_2^-)$
476	w	0.61	488	m	481	m	$\omega(PO_2^-)$
393	w	0.48	401	m			$t(PO_2^-)$
367	w	0.43	365	m			$\delta(OPO)$

* Raman and infrared frequencies (σ) are in cm^{-1} units. Intensities (I) are designated as s (strong), m (medium), w (weak), or sh (shoulder). Raman depolarization ratios (ρ) are defined in the text. Values in parentheses are estimates for very weak or poorly resolved bands.

‡ Abbreviations: ν, stretch; δ, bend; ω, wag; r, rock; t, twist; τ, torsion; s, symmetric; a, asymmetric.

TABLE 2 Vibrational spectra and assignments of NaDMP-$^{13}C_2$*

Raman					Infrared		
Solution			Solid		Solid		
σ	I	ρ	σ	I	σ	I	Assignment
3010	w	(0.5)			3004	w	$\nu_a(^{13}CH_3)$
2987	w	(0.7)	2991	w			$\nu_a(^{13}CH_3)$
2953	s	0.01	2971	w	2970	w	$\nu_s(^{13}CH_3)$
			2945	m	2946	w	
2911	w	0.12	2909	sh	2906	w	
2852	s	0.01	2844	s	2845	w	
1462	m	0.75			1463	m	$\delta_a(^{13}CH_3)$
1444	m	0.41	1442	m			$\delta_s(^{13}CH_3)$
1211	w	0.72	1243	w	1241	s	$\nu_a(PO_2^-)$
1180	w	0.60			1178	m	$r(^{13}CH_3)$
1151	w	0.72					$r(^{13}CH_3)$
1083	s	0.04	1121	s	1117	s	$\nu_s(PO_2^-)$
1047	m	0.15	1077	m	1084	s	$\nu_s(^{13}CO)$
			1051	w	1049	s	
1026	sh	(0.5)	1021	w	1030	m	$\nu_a(^{13}CO)$
821	w	0.65	797	m	801	s	$\nu_a(OPO)$
751	s	0.01	747	s	747	m	$\nu_s(OPO)$
			736	w			
538	w	0.72	559	m	565		$r(PO_2^-)$
501	sh	0.49	524	m			$\delta(PO_2^-)$
471	w	0.60	483	m			$\omega(PO_2^-)$
390	w	0.48	397	m			$t(PO_2^-)$
368	w	0.57	363	m			$\delta(OPO)$

* Notation and abbreviations are as in Table 1.

Jayaram et al., 1988). Additional experimental and theoretical evidence in support of the *gg* conformer stability has been cited by Jayaram et al. (1988).

3. Spectral band assignments

The large spatial separation of the two methyl groups of DMP allows them to be considered as independent vibrating units, each ideally with local C_{3v} symmetry. In principle, one symmetric and one degenerate C-H stretching mode are expected in the Raman effect for a C_{3v} methyl group. In practice, however, the degenerate members are often inequivalent and can give rise to two closely spaced Raman bands, both of which are depolarized (Ven der Veken et al., 1986; Odeurs et al., 1984). The symmetric C-H stretching mode is distinguished by its polarized Raman band. Additionally, one symmetric deformation, one degenerate deformation, and one degenerate rocking mode are expected. The remaining seven atoms of DMP will generate eight symmetric and seven asymmetric vibrations (*gg* conformer), along with two low-frequency CH_3 torsions, all of which are Raman active.

a. Hydrogenic modes

The regions 2950–3100 cm^{-1} of the Raman spectra of DMP-h_6 (Fig. 2) and DMP-$^{13}C_2$ (Fig. 3) show the typical five-band pattern expected for C-H stretching vibrations of the methoxy group (Bellamy, 1968). The bands at 3021 and 2997 cm^{-1}, which are depolarized (Table 1), are assigned to the quasi-degenerate C-H stretching vibrations. The bands at 2958 and 2856 cm^{-1} exhibit nearly equivalent intensities and both are polarized, contrary to the expectation of only one intense and polarized Raman band in this region. The two polarized bands are assigned as a Fermi doublet, which is confirmed by empirical correlations (Colthup et al., 1990). In the case of DMP-h_6 (Fig. 2), the uncoupled frequencies of the Fermi doublet are calculated as 2915 and 2898 cm^{-1}. The lower member is very close to the overtone (2900) of the assigned symmetric CH_3 deformation fundamental (2×1450), while the higher frequency (2915) is considered as the uncoupled symmetric C-H stretching mode. Applying the same procedure to DMP-$^{13}C_2$ (Table 2), we obtain uncoupled frequencies of 2912 and 2893 cm^{-1}. Again, the lower frequency is close to the overtone (2888) of the symmetric $^{13}CH_3$ deformation fundamental (2×1444), and the higher frequency member (2912) is assigned as the fundamental. In the normal coordinate calculations discussed below, we have employed the uncoupled fundamental frequencies. The depolarization ratios in Table 3 and Raman and IR intensities in Fig. 4 suggest that the band of DMP-d_6 at 2088 cm^{-1} should be assigned to the symmetric C-D stretching mode, and the two nearby bands of higher frequency should be identified with the quasi-degenerate C-D stretching vibrations. These assignments are consistent with the assignment of C-D bands in deuterated dimethylmethoxyphosphine (Ven der Veken et al., 1986) and methyldimethylphosphinate (Odeurs et al., 1984).

Assignment of the bands of DMP-h_6 at 1450 and 1464 cm^{-1} to symmetric and degenerate CH_3 deformation modes,

TABLE 3 Vibrational spectra and assignments of NaDMP-d_6*

Raman					Infrared		
Solution			Solid		Solid		
σ	I	ρ	σ	I	σ	I	Assignment
2273	m	0.75					$\nu_a(CD_3)$
2252	sh	(0.5)	2249	w	2260	w	$\nu_a(CD_3)$
			2234	sh	2233	w	
2214	m	0.05	2216	w	2214	w	
2176	sh	0.06					
2141	m	0.04	2133	m	2132	w	
2088	s	0.04	2079	s	2078	w	$\nu_s(CD_3)$
1213	w	0.69	1245	w	1241	s	$\nu_a(PO_2^-)$
1122	m	0.12	1143	m	1133	s	$\delta_s(CD_3)$
			1106	w	1098	w	
1082	m	0.11	1078	w	1071	s	$\nu_s(PO_2^-)$
1056	s	0.18	1057	w			$\nu_s(CO)$
			1044	w	1044	s	$\nu_a(CO)$
			1008	w	979	w	
					971	w	
932	m	0.15	928	m	936	w	$r(CD_3)$
900	w	(0.8)	899	m	902	w	$r(CD_3)$
					879	w	
					863	w	
786	w	0.68	763	m	763	s	$\nu_a(OPO)$
724	s	0.05	722	s	720	m	$\nu_s(OPO)$
527	m	(0.6)	550	m	535	w	$r(PO_2^-)$
			516	m	524	w	
485	sh	(0.4)	480	m			$\delta(PO_2^-)$
465	m	0.70					$\omega(PO_2^-)$
382	m	0.39	390	m			$t(PO_2^-)$
362	m	0.54	359	m			$\delta(OPO)$

* Notation and abbreviations are as in Table 1.

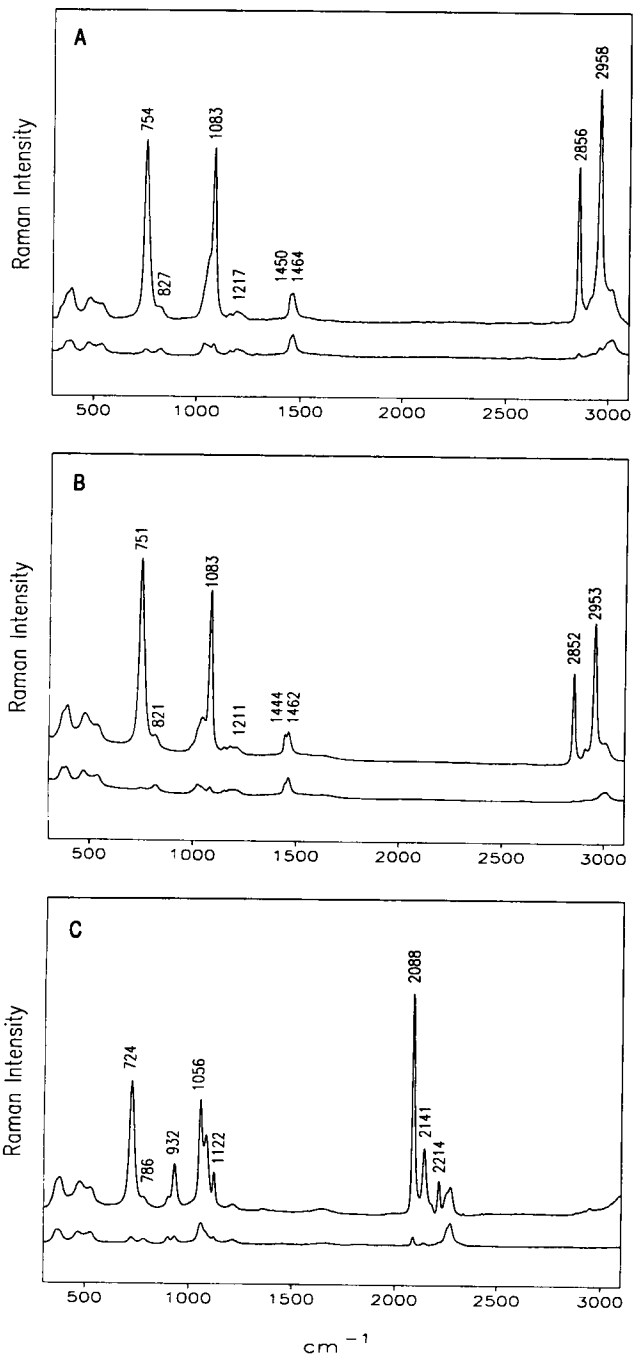

FIGURE 5 Perpendicular ($I_\perp$) and parallel ($I_\parallel$) components of the polarized Raman spectra of H_2O solutions of sodium dimethyl phosphate isotopomers, each at 0.8 M, pH 7.2. (*A*) NaDMP-h_6. (*B*) NaDMP-$^{13}C_2$. (*C*) NaDMP-d_6.

respectively, is straightforward, consistent with earlier assignments and empirical correlations (Colthup et al., 1990). In DMP-$^{13}C_2$, the corresponding frequencies are 1444 and 1462 cm^{-1}. In DMP-d_6, the symmetric and degenerate CD_3 deformations are presumably observed at 1143 (isotope shift = 1.26) and 1106 cm^{-1} (1.32), respectively. We note that the basis for assignment of the 1143 cm^{-1} band as the symmetric CD_3 deformation is the polarization of its counterpart at 1122 cm^{-1} (ρ = 0.12; Table 3) in the solution spectrum. Thus, the band at 1106 cm^{-1} may be reasonably assigned to the degenerate CD_3 deformation. The order of the frequencies of symmetric and degenerate CD_3 deformations is the reverse of that observed for the corresponding CH_3 deformation modes. Such frequency reversal of methyl deformations upon deuteration is observed in other phosphomethoxy derivatives (Ven der Veken et al., 1986). The degeneracy of methyl rocking vibrations, like that of C-H stretching and deformation vibrations, is removed in the DMP anion. The bands at 1192 and 1159 cm^{-1} of DMP-h_6, both of which are depolarized (Table 1), are assigned to asymmetric CH_3 rocking. The corresponding modes of DMP-$^{13}C_2$ and DMP-d_6 are observed, respectively, at 1180 and 1151 cm^{-1} (Table 2) and at 932 and 900 cm^{-1} (Table 3).

b. C—O stretching modes

In-phase and out-of-phase C—O stretching modes are expected in *gg* dialkyl phosphate esters. Shimanouchi et al. (1964) assigned bands near 1040 and 1056 cm^{-1} in solutions of $Ba(DMP)_2$ and NaDMP to C—O stretching but did not identify the symmetries of the vibrations. Garrigou-Lagrange et al. (1976) assigned Raman bands at 1064 and 1045 cm^{-1} in NaDMP to asymmetric and symmetric C—O stretching, respectively. In recent vibrational analyses of DMP crystals, Taga et al. (1991) assigned only one band at 1048 cm^{-1} to C—O stretching in $Ba(DMP)_2$, although two different C—O

stretching frequencies were calculated for each conformer (*gg*, *gt*, *tt*). The symmetry of the band at 1048 cm^{-1} was not determined by these authors.

In Fig. 6 *A* we show enlargements of the polarized Raman spectrum of DMP-h_6 solution in the region of the expected C—O stretching vibrations. In each case the complex band envelope is decomposed into the minimum number of Lorentzian components. The measured depolarization ratios (Table 1) indicate that in DMP-h_6 the polarized band at 1058 cm^{-1} is most probably due to in-phase C—O stretching, and the depolarized band at 1037 cm^{-1} is consistent with an out-of-phase mode. Isotope shifts in DMP-$^{13}C_2$, particularly the displacement of the overlapping band near 1083 cm^{-1} (Fig. 6 *B*), facilitate more accurate measurement of the depolarization ratios of the ^{13}C—O stretching bands, which occur at 1047 and 1026 cm^{-1} (Table 2). The frequencies and depolarization ratios in DMP-$^{13}C_2$ are consistent with our proposed assignments for DMP-h_6. In DMP-d_6, only one putative C—O stretching band is observed, at 1056 cm^{-1} (ρ = 0.18; Table 3). The depolarized counterpart is presumably overlapped by other more intense bands shifted into the 1000–1100 cm^{-1} region by methyl deuteration (Fig. 4). We note that our assignments compare very favorably with those given for symmetric (1050) and asymmetric (1037 cm^{-1}) modes of *O,O*-dimethylphosphorothioic acid and related model compounds (Nyquist, 1969). To support the experimentally determined assignments, we carried out *ab initio* calculations on the DMP anion (Y. Guan, R. Glaser, and G. J. Thomas, Jr., manuscript in preparation). The calculations support the assignment of the in-phase C—O stretching vibration at higher frequency than the out-of-phase mode. Specifically, the calculated values (scaling factor = 0.85) are 1061.4 (ρ = 0.17) and 1049.3 cm^{-1} (ρ = 0.75), in good agreement with the assignments of Table 1.

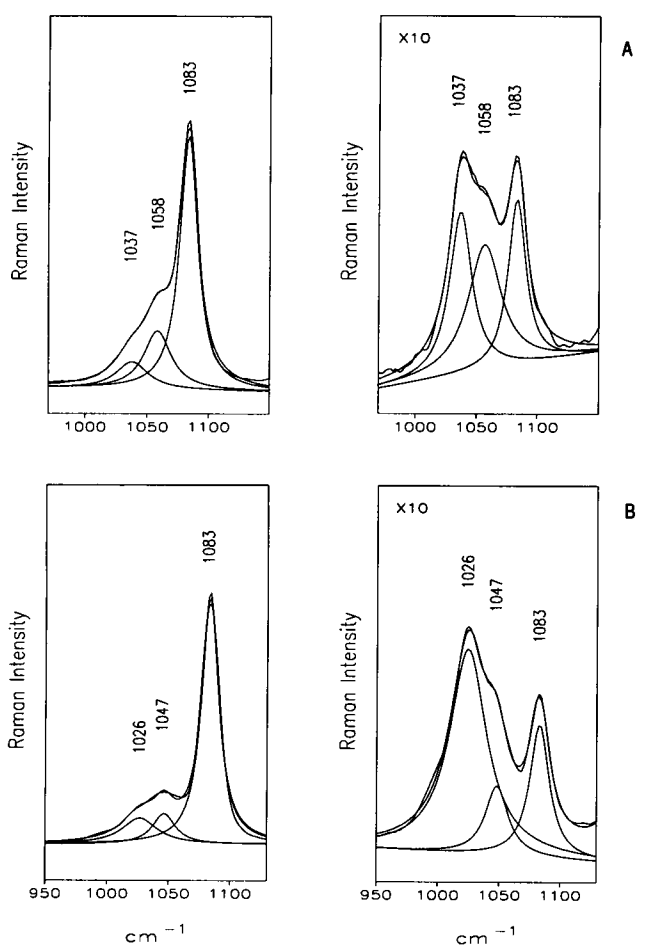

FIGURE 6 Perpendicular (*right*) and parallel (*left*) polarized Raman spectra of dimethyl phosphate isotopomers in the region of C—O stretching vibrations. (*A*) NaDMP-h_6. (*B*) NaDMP-$^{13}C_2$. In each panel the complex band envelope is fitted to the minimum number of Lorentzian components which accurately reproduce the observed spectral profile.

c. Phosphate stretching modes

The bands of DMP-h_6 at 1217 and 1083 cm^{-1} are assigned, respectively, to asymmetric and symmetric phosphorus-oxygen (P–O) stretching vibrations of the phosphodioxy group (PO_2^-). As expected, the symmetrical mode is polarized and intense in the Raman, while the asymmetric mode is depolarized and weak in the Raman but intense in the infrared. Neither band is substantially shifted by ^{13}C or ^{2}H substitution (Tables 1–3).

Mixing of the stretching modes of the ester oxygen-phosphorus bonds (O—P—O) is expected. In DMP-h_6, the Raman band at 754 cm^{-1} is highly polarized and very strong, whereas the band at 827 cm^{-1} is depolarized and weak (Table 1). Thus, we assign these, respectively, to vibrations that are substantially in-phase and out-of-phase oxygen-phosphorus stretching vibrations of the O—P—O diester group. The corresponding modes occur in DMP-$^{13}C_2$ at 751 and 821 cm^{-1} (Table 2) and in DMP-d_6 at 724 and 786 cm^{-1} (Table 3). These data show that O—P—O modes are affected both by ^{2}H and ^{13}C isotope substitutions, implying some mixing with vibrations of the methoxy moieties.

d. Phosphate deformation modes

Five Raman bands attributable to bending modes of the dialkyl phosphate group are observed in the region 300–600 cm^{-1} (Table 1–3). The observed depolarization ratios imply that the bands at 539 cm^{-1} and 476 cm^{-1} are due to asymmetric vibrations. We assign the former to O–P–O rocking and the latter to O–P–O wagging of the PO_2^- group. The weak band at 520 cm^{-1} in the IR spectrum is assigned to symmetric O–P–O bending because its presumed Raman counterpart (503 cm^{-1}) is polarized. The polarized Raman band at 393 cm^{-1} is assigned to O–P–O twisting. The remaining polarized Raman band at 367 cm^{-1} is assigned to O—P—O bending of the phosphodiester group. Spectral assignments for DMP-$^{13}C_2$ and DMP-d_6 in this region are essentially identical to those for DMP-h_6. Although Fourier transform infrared (FTIR) spectra below 400 cm^{-1} (KBr cutoff) and Raman spectra below 300 cm^{-1} (H_2O interference)

could not be obtained, we expect two P—O—C bending modes, two P—O torsions, and two C—O torsions below 400 cm^{-1}.

4. Normal coordinate calculations

Internal coordinates of the *gg* conformer of the DMP anion are shown in Fig. 7. With each atom of DMP considered as a single dynamic unit, 17 symmetry coordinates of symmetry species *A* and 16 of species *B* were constructed (Table 4). Initial values of the GVFF force constants, converted from UBFF calculations, are given in the second column of Table 5. In the course of refining these force constants, we found that a good fit of all observed and calculated frequencies of all isotopomers could not be obtained with a single set of hydrogenic stretching force constants, although other modes were in satisfactory agreement. Accordingly, we refined separately the C-D stretching force constant and the C-D/C-D interaction force constant to improve the fit between calculated and observed frequencies of the deuteriomethyl groups of DMP-d_6. The refined force constants are given in the third column of Table 5. Tabulations of the observed and calculated frequencies are given in Table 6 (DMP-h_6), Table 7 (DMP-$^{13}C_2$), and Table 8 (DMP-d_6).

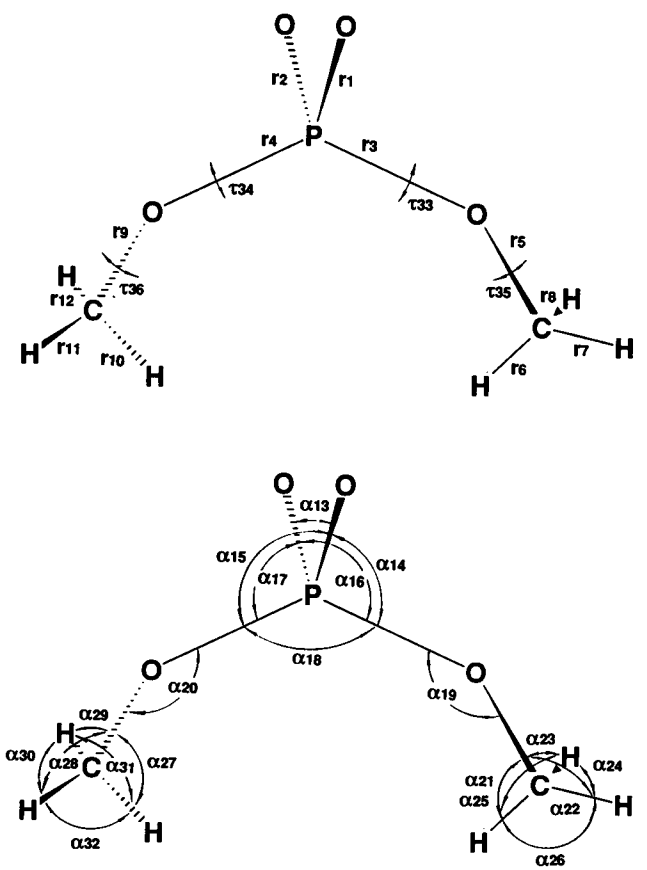

FIGURE 7 Internal coordinates of the *gg* conformer of dimethyl phosphate anion. *Top:* Stretching and torsion coordinates. *Bottom:* Bending coordinates.

TABLE 4 Symmetry coordinates of dimethyl phosphate*

Species	Symmetry coordinate	Description
A	S1 = r1 + r2	$\nu_s(PO_2^-)$
	S2 = r3 + r4	$\nu_s(OPO)$
	S3 = r5 + r9	$\nu_s(CO)$
	S4 = r6 + r7 + r8 + r10 + r11 + r12	$\nu_s(CH_3)$
	S5 = 2r6 − r7 − r8 + 2r10 − r11 − r12	$\nu_a(CH_3)$
	S6 = α13	$\delta(PO_2^-)$
	S7 = α18	δ(OPO)
	S8 = α19 + α20	δ_s(POC)
	S9 = 2α21 − α22 − α23 + 2α27 − α28 − α29	r(CH_3)
	S10 = α21 + α22 + α23 − α24 − α25 − α26 + α27 + α28 + α29 − α30 − α31 − α32	$\delta_s(CH_3)$
	S11 = −α24 − α25 + 2α26 − α30 − α31 + 2α32	$\delta_a(CH_3)$
	S12 = τ33 + τ34	τ_s(OPOC)
	S13 = τ35 + τ36	τ_s(POCH)
	S14 = r7 − r8 + r11 − r12	$\nu_a(CH_3)$
	S15 = α14 − α15 − α16 + α17	t(PO_2^-)
	S16 = α22 − α23 + α28 − α29	r(CH_3)
	S17 = α24 − α25 + α30 − α31	$\delta_a(CH_3)$
B	S1 = r1 − r2	$\nu_a(PO_2^-)$
	S2 = r3 − r4	ν_a(OPO)
	S3 = r5 − r9	ν_a(CO)
	S4 = r6 + r7 + r8 − r10 − r11 − r12	$\nu_s(CH_3)$
	S5 = 2r6 − r7 − r8 − 2r10 + r11 + r12	$\nu_a(CH_3)$
	S6 = α14 − α15 + α16 − α17	ω(PO_2^-)
	S7 = α19 − α20	δ_a(POC)
	S8 = α22 − α23 − α28 + α29	r(CH_3)
	S9 = α24 − α25 − α30 + α31	$\delta_a(CH_3)$
	S10 = r7 − r8 − r11 + r12	$\nu_a(CH_3)$
	S11 = α14 + α15 − α16 − α17	r(PO_2^-)
	S12 = 2α21 − α22 − α23 − 2α27 + α28 + α29	r(CH_3)
	S13 = α21 + α22 + α23 − α24 − α25 − α26 − α27 − α28 − α29 + α30 + α31 + α32	$\delta_s(CH_3)$
	S14 = −α24 − α25 + 2α26 + α30 + α31 − 2α32	$\delta_a(CH_3)$
	S15 = τ33 − τ34	τ_a(OPOC)
	S16 = τ35 − τ36	τ_a(POCH)

* Symmetry coordinates are unnormalized. Notation is defined in Table 1 and Fig. 7.

a. Anharmonicity of hydrogen stretching modes

As noted in Table 5, the hydrogenic stretching force constant increases by 3% with deuteration, from 4.953 mdyn/Å in DMP-h_6 to 5.127 mdyn/Å in DMP-d_6. Similar results, attributable to greater anharmonicity in C-H isotopomers (Wilson et al., 1955), have been obtained for other methyl-containing structures. In a recent study, Fischer et al. (1991) report a 2.6% increase in the C-H stretching force constant with deuteration of methyl substituents, due to lesser anharmonicity of the C-D stretching vibrations.

b. C—O stretching/interaction force constants

The fit between observed and calculated frequencies of each DMP isotopomer was improved in the GVFF by incorporation of a single nonbonded interaction force constant, namely that of interaction between the two C—O stretching coordinates, for which a refined value of 0.108 mdyn/Å was obtained. The initial value of this force constant (0.025 mdyn/Å; Table 5) was transferred from an *ab initio* treatment of the DMP anion (Y. Guan, R.

TABLE 5 Generalized valence force field of dimethyl phosphate

Force constant	Initial value*	Refined value‡
Stretching (mdyn/Å)		
P–O	8.535	8.541
P—O	4.710	4.928
C—O	4.773	4.693 (4.677)
C-H	4.951	4.953 (5.127)
Bending (mdyn Å/rad²)		
O–P–O	1.384	1.510
O–P—O	1.783	1.446
O—P—O	1.938	1.490
P—O—C	0.710	0.705
O—C-H	0.895	0.879
H-C-H	0.523	0.572
Torsion (mdyn Å/rad²)		
O—P—O—C‖	0.080	0.080
P—O—C-H‖	0.038	0.038
Stretching/stretching (mdyn/Å)		
P–O/P–O	0.041	0.725
P–O/P—O	0.390	0.673
P—O/P—O	0.691	0.316
P—O/O—C	0.232	0.094
O—C/C-H	0.521	0.555
C-H/C-H	0.050	0.005 (–0.033)
C—O/C—O§	0.025	0.108 (0.109)
Bending/bending (mdyn/rad)		
P–O/O–P–O‖	0.357	0.357
P–O/O–P—O‖	0.359	0.359
O—P/O–P—O‖	0.378	0.378
O—P/O—P—O‖	0.380	0.380
P—O/P—O—C‖	0.184	0.184
O—C/P—O—C‖	0.173	0.173
O—C/O—C-H‖	0.441	0.441
C-H/O—C-H	0.345	0.214
C-H/H-C-H	0.093	0.340
Bending/bending (mdyn Å/rad²)		
O–P–O/O–P—O‖	0.264	0.264
O–P—O/O—P—O‖	0.264	0.264
O—C-H/H-C-H	0.015	0.048
O–P–O/O—P—O	0.374	0.130
O–P—O/O–P—O	0.264	–0.189
O–P—O/O—P–O	0.374	–0.383
O—C-H/O—C-H	0.015	0.042
O—C-H/H-C-H‖	–0.013	–0.013

* Obtained from Urey-Bradley force field. See text.
‡ Values in parentheses are for DMP-d_6. See text.
§ Obtained from *ab initio* calculation. See text.
‖ Indicates that the value of the force constant was fixed in the calculation.

TABLE 6 Observed and calculated frequencies of DMP-h_6*

σ_{obs}	σ_{calc}	Assignment	PED(%)‡
3021	3021	$\nu_a(CH_3)$	C-H (100)
3021	3020	$\nu_a(CH_3)$	C-H (100)
2915§	2914	$\nu_s(CH_3)$	C-H (100)
1464	1464	$\delta_a(CH_3)$	H-C-H (95)
1464	1463	$\delta_a(CH_3)$	H-C-H (95)
1450	1448	$\delta_s(CH_3)$	O—C-H (60, H-C-H (34)
1217	1218	$\nu_a(PO_2^-)$	P–O (95)
1192	1188	$r(CH_3)$	O—C-H (94)
1159	1162	$r(CH_3)$	O—C-H (94)
1083	1084	$\nu_s(PO_2^-)$	P–O (92)
1058	1059	$\nu_s(CO)$	C—O (81), P–O (14)
1037	1040	$\nu_a(CO)$	C—O (81), P—O (18)
827	826	$\nu_a(OPO)$	P—O (66), C—O (20)
754	761	$\nu_s(OPO)$	P—O (67), C—O (20)
539	549	$r(PO_2^-)$	O—P–O (72)
503	504	$\delta PO_2^-)$	O–P–O (67), P—O (30)
476	476	$\omega(PO_2^-)$	O—P–O (62)
393	396	$t(PO_2^-)$	O—P–O (76), P—O—C (20)
367	368	$\delta(OPO)$	O—P—O (38), O–P–O (27)
(241)‖	233	$\delta_a(POC)$	P—O—C (83)
(218)‖	205	$\delta_s(POC)$	P—O—C (63), O—P—O (19)
	166	$\tau_a(CO)$	P—O—C-H (70), O—P—O—C (25)
(148)‖	142	$\tau_s(CO)$	P—O—C-H (94)
(108)‖	108	$\tau_a(PO)$	O—P—O—C (73), P—O—C-H (26)
(75)‖	72	$\tau_s(PO)$	O—P—O—C (94)

Average error: 4.09 cm^{-1}

* Notation is defined in Table 1.
‡ Potential energy distribution in terms of force constants.
§ Fermi doublet member. The uncoupled frequency was used in the calculation.
‖ Data of Taga et al. (1991); not used in the calculations.

Glaser, and G. J. Thomas, Jr., manuscript in preparation). Omission of the C—O/C—O interaction constant results in calculated out-of-phase and in-phase C—O stretching frequencies which are, respectively, 10 cm^{-1} higher and lower than the values observed in all isotopomers. Although incorporation of the C—O/C—O interaction term in the GVFF implies interaction between the two ester bonds, we believe this term is justified by the significantly improved fit between observed and calculated frequencies of each DMP isotopomer.

c. Uncoupling of alkyl and skeletal modes

In the present normal coordinate treatment we have considered each methyl group explicitly as a complete (C_{3v}) structural entity. The results confirm both decoupling of the two methyl groups from one another and decoupling of methyl group vibrations from those of the phosphodiester skeleton. Accordingly, in Tables 6–8, frequencies of the *A* type and *B* type modes of the methyl group are identical.

d. Reversal of deuteriomethyl deformation modes

The proposed frequency reversal of methyl deformation modes upon deuteration (Results and Discussion, Section 3.a.) is confirmed by the normal coordinate calculations. Calculated values of the symmetric and degenerate CD_3 deformations are 1101 and 1065 cm^{-1}, compared with calculated values of 1448 and 1463 cm^{-1} for the respective CH_3 modes. Durig et al. (1991) reported a similar reversal for CD_3 deformations of 2-fluoropropane, supported by normal coordinate and *ab initio* calculations.

SUMMARY AND CONCLUSIONS

Normal mode assignments for the phosphodiester group of the dimethyl phosphate anion in the *gg* conformation have been established by analysis of the infrared and Raman spectra of $(CH_3O)_2PO_2^-$, $(CD_3O)_2PO_2^-$, and $(^{13}CH_3O)_2PO_2^-$. Vibrational spectra of both solids and aqueous solutions have been considered. Raman depolarization ratios, which provide key information for resolving previously ambiguous assignments, are reported for all major Raman bands in solution

TABLE 7 Observed and calculated frequencies of DMP-$^{13}C_2$*

σ_{obs}	σ_{calc}	Assignment	PED(%)
3010	3011	$\nu_a(^{13}CH_3)$	^{13}C-H (100)
3010	3011	$\nu_a(^{13}CH_3)$	^{13}C-H (100)
2912‡	2914	$\nu_s(^{13}CH_3)$	^{13}C-H (100)
1462	1461	$\delta_a(^{13}CH_3)$	H-^{13}C-H (95)
1462	1460	$\delta_a(^{13}CH_3)$	H-^{13}C-H (95)
1444	1443	$\delta_s(^{13}CH_3)$	O—^{13}C-H (60), H-^{13}C-H (34)
1211	1217	$\nu_a(PO_2^-)$	P–O (95)
1180	1180	$r(^{13}CH_3)$	O—^{13}C-H (94)
1151	1154	$r(^{13}CH_3)$	O—^{13}C-H (94)
1083	1084	$\nu_s(PO_2^-)$	P–O (92)
1047	1044	$\nu_s(^{13}CO)$	^{13}C—O (84), P–O (11)
1026	1026	$\nu_a(^{13}CO)$	^{13}C—O (74), P—O (18)
821	819	ν_a(OPO)	P—O (62)
751	756	ν_s(OPO)	P—O (67), ^{13}C—O (24)
538	550	$r(PO_2^-)$	O—P–O (78)
501	504	$\delta(PO_2^-)$	O–P–O (54), O—P—O (30)
471	460	$\omega(PO_2^-)$	O—P–O (78)
390	396	$t(PO_2^-)$	O—P–O (73), O—P—O (17)
368	365	δ(OPO)	O—P—O (46), O–P–O (30)
	230	$\delta_a(PO^{13}C)$	P—O—^{13}C (78)
	202	$\delta_s(PO^{13}C)$	P—O—^{13}C (63), O—P—O (19)
	165	$\tau_a(^{13}CO)$	P—O—^{13}C-H (70), O—P—O—^{13}C (25)
	141	$\tau_s(^{13}CO)$	P—O—^{13}C-H (90)
	108	τ_a(PO)	O—P—O—^{13}C (73), P—O—^{13}C-H (26)
	71	τ_s(PO)	O—P—O—^{13}C (94)

Average error: 4.09 cm^{-1}

* Notation is defined in Table 6.

‡ Fermi doublet member. The uncoupled frequency was used in the calculation.

TABLE 8 Observed and calculated frequencies of DMP-d_6*

σ_{obs}	σ_{calc}	Assignment	PED(%)+
2273	2273	$\nu_a(CD_3)$	C-D (100)
2273	2273	$\nu_a(CD_3)$	C-D (100)
2088	2088	$\nu_s(CD_3)$	C-D (100)
1213	1216	$\nu_a(PO_2^-)$	P–O (95)
	1101	$\delta_s(CD_3)$	O—C-D (54), D-C-D (29)
1082	1086	$\nu_s(PO_2^-)$	P–O (93)
	1068	$\delta_a(CD_3)$	D-C-D (95)
	1065	$\delta_a(CD_3)$	D-C-D (95)
1056	1056	ν_s(CO)	C—O (45), P—O (41)
	1051	ν_a(CO)	C—O (44), P—O (42)
932	942	$r(CD_3)$	O—C-D (71), C—O (18)
900	904	$r(CD_3)$	O—C-D (94)
786	782	ν_a(OPO)	P—O (53), O—C-D (20)
724	718	ν_s(OPO)	P—O (45), O—C-D (24)
527	537	$r(PO_2^-)$	O—P–O (74)
485	492	$\delta(PO_2^-)$	O–P–O (55), P—O (27)
465	455	$\omega(PO_2^-)$	O—P–O (68)
382	388	$t(PO_2^-)$	O—P–O (73), P—O–C (22)
362	357	δ(OPO)	O—P—O (46), O–P–O (27)
	212	δ_a(POC)	P—O—C (81)
	188	δ_s(POC)	P—O—C (70)
	140	τ_a(C—O)	P—O—C-D (49), O—P—O—C (46)
	103	τ_s(C—O)	P—O—C-D (90) O—C (46)
	85	τ_a(P—O)	O—P—O—C (51), P—O—C-D (48)
	63	τ_s(P—O)	O—P—O—C (92)

Average error: 8.54 cm^{-1}

* Notation is defined in Table 6.

spectra of the three DMP isotopomers. We have combined the experimental results with *ab initio* calculation of force constants to develop a generalized valence force field for the C—O—P—O—C phosphodiester network. The GVFF force field satisfactorily reproduces the experimentally observed vibrational frequencies of the three DMP isotopomers. The results are considered a first step toward the development of satisfactory force fields for the phosphodiester backbones of DNA and RNA. The principal conclusions reached from this study are as follows:

1. In-phase [ν_s(CO)] and out-of-phase [ν_a(CO)] stretching vibrations of the diester linkages have been identified (Tables 1–3), on the basis of the experimentally determined isotope shifts and Raman depolarization ratios in spectra of DMP-h_6, DMP-$^{13}C_2$, and DMP-d_6. In the normal isotopomer (DMP-h_6), we observe ν_s(CO) = 1058 and ν_a(CO) = 1037 cm^{-1}, with the former polarized and latter depolarized. The occurrence of ν_s(CO) > ν_a(CO) is confirmed in ^{2}H and ^{13}C derivatives.

2. A single, nonbonded, off-diagonal force constant in the generalized valence force field is sufficient to reproduce the experimentally observed vibrational frequencies. This force constant, derived from the *ab initio* treatment, corresponds to nonbonded interaction of the two C—O bonds.

3. Specific assignments have been made for the nine stretching and bending modes of the phosphodioxy (O–P–O) and phosphodiester (O—P—O) groups of DMP. These assignments confirm and extend earlier studies that focused on selected symmetrical modes of the dialkyl phosphate moiety (Shimanouchi et al., 1964; Brown and Peticolas, 1975).

4. Relatively large anharmonic effects depress the effective GVFF force constant for carbon-hydrogen stretching vibrations in DMP-h_6 and DMP-$^{13}C_2$. The absence of comparable anharmonicity in deuteriomethyl C-D stretching modes of DMP-d_6 is dealt with in the normal coordinate analysis by increasing the corresponding C-D stretching force constant by approximately 3%. These findings are consistent with results reported for other methyl-containing structures.

5. The present results demonstrate decoupling of vibrations of the two methyl groups of DMP from one another. Our analysis also shows that methyl group modes are not strongly coupled to vibrations of the phosphodiester skeleton. The latter finding validates the approximation of treating each alkyl group of DMP as a single dynamic unit, a simplification that could be useful in studies of more complex dialkyl phosphate esters.

6. We observe a frequency reversal of the symmetric and degenerate methyl group deformations upon deuteration of dimethyl phosphate. This reversal is also supported by the normal coordinate analyses of DMP-h_6 and DMP-d_6. Similar reversals have been reported for other methyl-containing structures.

The comprehensive force field developed here for the DMP anion satisfactorily reproduces the vibrational frequencies observed for all isotopomers. Our results support the large body of evidence from other sources for the prevalence of the *gg* conformer ($\tau \approx 60°$, $\tau' \approx 60°$; Fig. 7) of DMP in solution. This force field should be useful as a starting point in normal coordinate analyses of other conformers of the dimethyl phosphate anion and should also be productive in

future normal coordinate analyses of additional phosphodiester analogs of DNA.

Conclusion 1, above, advances our understanding of the vibrational spectra of nucleic acids. A complex band of moderate intensity near 1050–1060 cm^{-1} has also been observed in DNA, RNA, and synthetic oligonucleotides and had been proposed as being due to CO stretching vibrations originating in the furanose-phosphate backbone (Prescott et al., 1984). The frequency, intensity, and polarization properties of the DNA Raman band (Benevides et al., 1993) all point to a vibrational origin similar to that determined here for DMP, namely, phosphoester C—O stretching. We note also that the nucleic acid Raman band near 1050–1060 cm^{-1} is conformationally sensitive (Prescott et al., 1984; Thomas and Benevides, 1985), and could serve as an indicator of backbone geometry. In future work we shall further investigate the dependency of the ν_s(CO) and ν_a(CO) stretching vibrations upon valence bond angles and torsion angles of the diester linkages, specifically in dialkyl phosphates, which more closely approximate the furanosyl 3′ and 5′ linkages of nucleic acids. Recent normal coordinate calculations predict substantial dependence of the skeletal stretching modes of dialkyl phosphates on the phosphodiester torsion angles, α and ζ, which define the configuration of phosphodiester groups in the backbone of double-helical nucleic acids (Y. Guan and G. J. Thomas, Jr., unpublished results). These findings will be presented in a future publication.

Conclusion 3, above, provides new insights into potentially useful Raman markers of the DNA phosphate groups. Recent studies reveal extraordinary sensitivity of the phosphodioxy symmetric stretching vibration near 1090 cm^{-1} to packaging of a viral dsDNA chromosome (Aubrey et al., 1992). The Raman bands near 1090 cm^{-1} in spectra of DNA fragments (Duguid et al., 1993) and simple DNA phosphate analogs (Stangret and Savoie, 1992) are also highly sensitive in frequency and intensity to interactions with metal cations. The present assignment of low-frequency bending modes of the PO_2^- group in the dimethyl phosphate anion (Table 1), particularly the rocking (539), scissoring (503), wagging (476), and twisting (393 cm^{-1}) modes, suggest that the low-frequency region of the Raman spectrum of DNA may contain additional marker bands to serve as indicators of electrostatic binding between phosphates and biologically important cationic agents. Phosphate-metal interactions are also expected to perturb the electronic structure in ester linkages, which may account for the observed sensitivity of Raman bands near 830 cm^{-1} (OPO diester stretching) to DNA-metal complexation (Duguid et al., 1993).

We thank Prof. R. Glaser (University of Missouri–Columbia) and Prof. H. Takeuchi (Tohoko University) for providing computational programs for this project and assistance to Y. G. in their implementation. We also thank Mr. A. Toyama for assistance in computations and Prof. M. Tsuboi for helpful comments on the manuscript.

This research was supported by NIH grant AI18758. This project was assisted by a U.S./Japan Cooperative Science grant (NSF-INT9116242) to G. J. T.

REFERENCES

Aubrey, K. L., S. R. Casjens, and G. J. Thomas, Jr. 1992. Secondary structure and interactions of the packaged dsDNA genome of bacteriophage P22 investigated by Raman difference spectroscopy. *Biochemistry.* 31: 11835–11842.

Bellamy, L. J. 1968. Advances in Infrared Group Frequencies. Methuen and Co., Ltd., London.

Benevides, J. M., A. H.-J. Wang, G. A. van der Marel, J. H. van Boom, A. Rich, and G. J. Thomas, Jr. 1984. The Raman spectra of left-handed DNA oligomers incorporating adenine-thymine base pairs. *Nucleic Acids Res.* 12:5912–5925.

Benevides, J. M., A. H-J. Wang, A. Rich, Y. Kyogoku, G. A. van der Marel, J. H. van Boom, and G. J. Thomas, Jr. 1986. Raman spectra of single crystals of r(GCG)d(CGC) and d(CCCCGGGG) as models for A-DNA, their structure transitions in aqueous solution, and comparison with double-helical poly(dG):poly(dC). *Biochemistry.* 25:41–50.

Benevides, J. M., A. H-J. Wang, G. A. van der Marel, J. H. van Boom, and G. J. Thomas, Jr. 1988. Crystal and solution structures of the B-DNA dodecamer d(CGCAAATTTGCG) probed by Raman spectroscopy: heterogeneity in the crystal structure does not persist in the solution structure. *Biochemistry.* 27:931–938.

Benevides, J. M., M. Tsuboi, A. H-J. Wang, and G. J. Thomas, Jr. 1993. Local Raman tensors of double-helical DNA in the crystal: A basis for determining DNA residue orientations. *J. Am. Chem. Soc.* 115: 5351–5359.

Brown, E. B., and W. L. Peticolas. 1975. Conformational geometry and vibrational frequencies of nucleic acid chains. *Biopolymers.* 14:1259–1271.

Colthup, N. B., L. H. Daly, and S. E. Wiberley. 1990. Introduction to Infrared and Raman Spectroscopy. 3rd Edition. Academic Press, Inc., San Diego.

Duguid, J., V. A. Bloomfield, J. M. Benevides, and G. J. Thomas, Jr. 1993. Raman spectroscopy of DNA-metal complexes. I. Interactions and conformational effects of the divalent cations: Mg, Ca, Sr, Ba, Mn, Co, Ni, Cu, Pd, and Cd. *Biophys. J.* 65:1916–1928.

Durig, J. R., H. Nanaie, and G. A. Guirgis. 1991. Raman and infrared spectra, barriers to internal rotation, vibrational assignments and ab initio calculations on 2- fluoropropane. *J. Raman Spectrosc.* 22:155–168.

Erfurth, S. C., E. J. Kiser, and W. L. Peticolas. 1972. Determination of the backbone structure of nucleic acids and nucleic acid oligomers by laser Raman scattering. *Proc. Natl. Acad. Sci. USA.* 69:938–941.

Ezra, F. S., and R. L. Collin. 1973. The crystal structure of magnesium diethyl phosphate, $Mg[PO_2(OC_2H_5)_2]_2$. *Acta Cryst.* B29:1398–1403.

Fischer, D., K. Klostermann, and K-L. Oehme. 1991. Raman spectra and normal coordinate analysis of thirteen selectively deuterated tetramethylsilanes. *J. Raman Spectrosc.* 22:19–30.

Garrigou-Lagrange, C., O. Bouloussa, and C. Clement. 1976. Analyse conformationnelle des dialkylphosphates. *Can. J. Spectrosc.* 21:75–82.

Giarda, L., F. Garbassi, and M. Calcaterra. 1973. The crystal structure of dimethyl ammonium phosphate, $NH_4(CH_3)_2PO_4$. *Acta Cryst.* B29: 1826–1829.

Jayaram, B., M. Mezei, and D. L. Beveridge. 1988. Conformational stability of dimethyl phosphate anion in water: liquid-state free energy simulations. *J Am. Chem. Soc.* 110:1691–1694.

Kyogoku, Y., and Y. Iitaka. 1966. The crystal structure of barium diethyl phosphate. *Acta Cryst.* 21:49–57.

Lafleur, L., J. Rice, and G. J. Thomas, Jr. 1972. Raman spectral studies of nucleic acids. VII. Poly(rA):poly(rU) and poly(rG):poly(rC). *Biopolymers.* 11:2423–2437.

Li, Y., G. J. Thomas, Jr., M. Fuller, and J. King. 1981. Investigations of bacteriophage P22 by laser Raman spectroscopy. *Prog. Clin. Biol. Res.* 64:271–283.

McIvor, R. A., G. D. McCarthy, and G. A. Grant. 1956. Preparation and toxicity of some alkyl thiopyrophosphates. *Can. J. Chem.* 34:1819–1832.

Mortimer, F. S. 1957. Vibrational assignment and rotational isomerism in some simple organic phosphates. *Spectrochim. Acta.* 9:270–281.

Newton, M. D. 1973. A model conformational study of nucleic acid phosphate ester bonds. The torsional potential of dimethyl phosphate monoanion. *J. Am. Chem. Soc.* 95:256–258.

Nishimura, Y., M. Tsuboi, T. Nakano, S. Higuchi, T. Sato, T. Shida, S.

Uesugi, E. Ohtsuka, and M. Ikehara. 1983. Raman diagnosis of nucleic acid structure: sugar puckering and glycosidic conformation in the guanosine moiety. *Nucleic Acids Res.* 11:1579–1588.

Nishimura, Y., and M. Tsuboi. 1986. Local conformations and polymorphism of DNA duplexes as revealed by their Raman spectra. *In* Advances in Spectroscopy. Vol. 13. Spectroscopy of Biological Systems. R. J. H. Clark and R. E. Hester, editors. Wiley, New York. 177–232.

Noller, C. R., and G. R. Dutton. 1933. Note on the preparation of trialkyl phosphates and their use as alkylating agents. *J. Am. Chem. Soc.* 55: 424–425.

Nyquist, R. A. 1969. Vibrational spectroscopic study of organophosphorus compounds: P-S-H and P-H groups. *Spectrochim. Acta.* 25A:47–66.

Odeurs, R. L., B. J. van der Veken, M. A. Herman, and J. R. Durig. 1984. Gas phase vibrational and conformational analysis of methyldimethylphosphinate and isotopically substituted derivatives. *J. Mol. Struct.* 117: 235–245.

Okabayashi, H., T. Yoshida, T. Ikeda, H. Matsuura, and T. Kitagawa. 1982. PO_2^- symmetric-stretching Raman line and molecular aggregation states of barium dialkyl phosphates. *J. Am. Chem. Soc.* 104:5399–5402.

Peticolas, W. L., W. L. Kubasek, G. A. Thomas, and M. Tsuboi. 1987. Nucleic acids. *In* Biological Applications of Raman Spectroscopy. Vol. 1. Raman Spectra and the Conformations of Biological Macromolecules. T. G. Spiro, editor. Wiley, New York. 81–133.

Prescott, B., W. Steinmetz, and G. J. Thomas, Jr. 1984. Characterization of DNA structures by laser Raman spectroscopy. *Biopolymers.* 23:235–256.

Shimanouchi, T., M. Tsuboi, and Y. Kyogoku. 1964. Infrared spectra of nucleic acids and related compounds. *Adv. Chem. Phys.* 7:435–498.

Small, E. W., and W. L. Peticolas. 1971. Conformational dependence of the Raman scattering intensities from polynucleotides. III. Order-disorder changes in helical structures. *Biopolymers.* 10:1377–1416.

Stangret, J., and R. Savoie. 1992. Vibrational spectroscopic study of the interaction of metal ions with diethyl phosphate, a model for biological systems. *Can. J. Chem.* 70:2875–2883.

Taga, K., K. Miyagai, N. Hirabayashi, T. Yoshida, and H. Okabayashi. 1991. Vibrational spectra and normal coordinate analysis of barium dimethyl, diethyl and ethyl methyl phosphates. *J. Mol. Struct.* 245:1–11.

Thamann, T., R. C. Lord. A. H-J. Wang, and A. Rich. 1981. The high-salt form of poly(dG-dC):poly(dG-dC) is left-handed DNA: Raman spectra of crystals and solutions. *Nucleic Acids Res.* 9:5443–5457.

Thomas, G. J., Jr., G. C. Medeiros, and K. A. Hartman. 1971. The dependence of Raman scattering on the conformation of ribosomal RNA. *Biochem. Biophys. Res. Commun.* 44:587–592.

Thomas, G. J., Jr., J. M. Benevides, and B. Prescott. 1986. DNA and RNA structures in crystals, fibers and solutions by Raman spectroscopy with applications to nucleoproteins. *Biomol. Stereodyn.* 4:227–254.

Thomas, G. J., Jr. 1987. Viruses and nucleoproteins. *In* Biological Applications of Raman Spectroscopy. Vol. 1. Raman Spectra and the Conformations of Biological Macromolecules. T. G. Spiro, editor. Wiley, New York. 135–201.

Thomas, G. J., Jr., and J. M. Benevides. 1985. An A-helix structure for poly(dA-dT) · poly(dA-dT). *Biopolymers.* 24:1101–1105.

Thomas, G. J., Jr., and A. H.-J. Wang. 1988. Laser Raman spectroscopy of nucleic acids. *In* Nucleic Acids and Molecular Biology. Vol. 2. F. Eckstein and D. M. J. Lilley, editors. Springer-Verlag, Berlin. 1–30.

Thomas, G. J., Jr., and M. Tsuboi. 1993. Raman Spectroscopy of Nucleic Acids and Their Complexes. *Adv. Biophys. Chem.* 3:1–69.

Ven der Veken, B. J., T. S. Little, Y. S. Li, M. E. Harris, and J. R. Durig. 1986. Spectra and structure of organophosphorus compounds. XXVIII. Vibrational and conformational analysis of dimethylmethoxyphosphine and some isotopically substituted derivatives. *Spectrochim. Acta.* 42A: 123–140.

Wilson, E. B., Jr., J. C. Decius, and P. C. Cross. 1955. Molecular Vibrations. McGraw-Hill, New York.